Cell Reports, Volume *29*

Supplemental Information

The Axonal Membrane Protein PRG2 Inhibits PTEN and Directs Growth to Branches

Annika Brosig, Joachim Fuchs, Fatih Ipek, Cristina Kroon, Sandra Schrötter, Mayur Vadhvani, Alexandra Polyzou, Julia Ledderose, Michiel van Diepen, Hermann-Georg Holzhütter, Thorsten Trimbuch, Niclas Gimber, Jan Schmoranzer, Ivo Lieberam, Christian Rosenmund, Christian Spahn, Patrick Scheerer, Michal Szczepek, George Leondaritis, and Britta J. Eickholt

Supplemental Figure S1

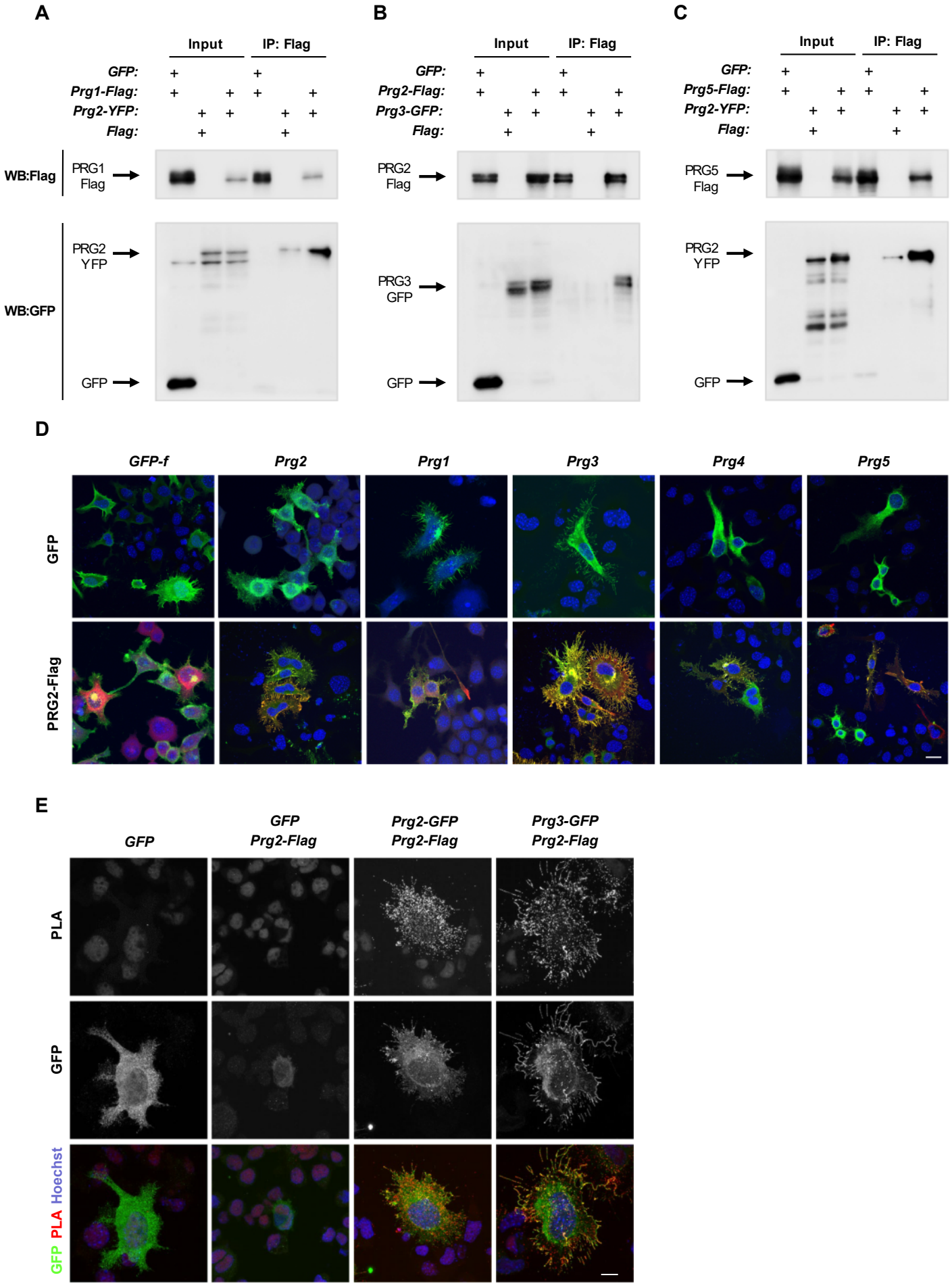

Supplemental Figure S1

PRG2 interacts and multimerizes at the plasma membrane with other members of the PRG-family, Related to Figure 1

PRG2 interacts with other PRG-family members in N1E cells. (**A**) PRG2-YFP co-immunoprecipitates with PRG1-Flag, (**B**) PRG3-GFP co-immunoprecipitates with PRG2-Flag and (**C**) PRG2-YFP co-immunoprecipitates with PRG5-Flag (**D**) All PRG-family members localize to endoplasmic reticulum as well as plasma membrane when expressed individually. Coexpression of PRG-family members with PRG2-Flag shows co-localization as well as enhanced plasma membrane recruitment of PRGs. Scale bar = 20 μm. (**E**) Proximity-ligation assays show direct interaction of PRG2-homomultimers as well as PRG2-PRG3 heteromultimers particularly at the plasma membrane and filopodia. Scale bar = 20 μm.

Supplemental Figure S2

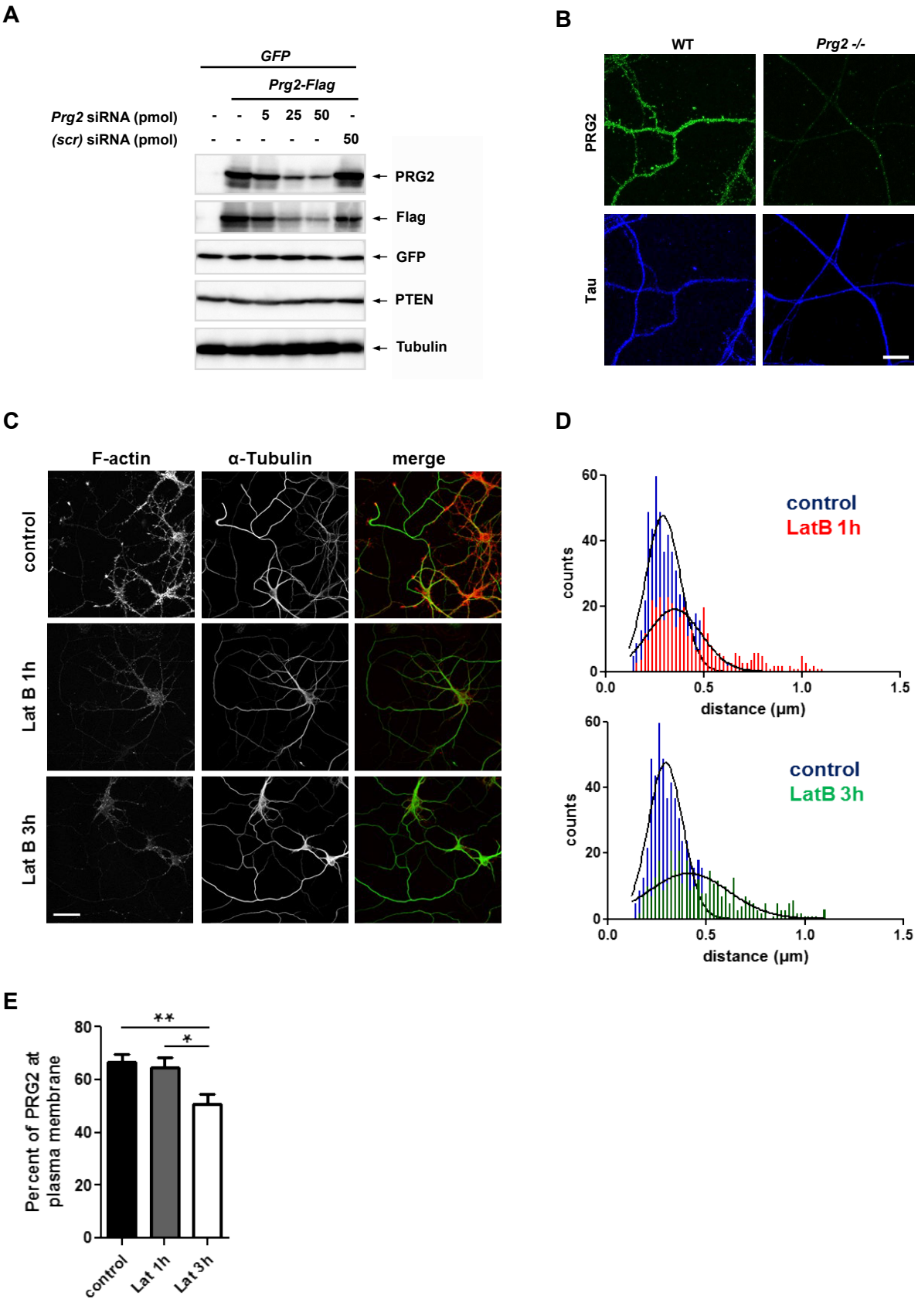

Supplemental Figure S2

Characterization of the custom-made PRG2 antibody, Related to Figure 4

(**A**) *Prg2-Flag* (and control *GFP*) was expressed in HEK293 cells in the presence of *Prg2* siRNA or non-targeting siRNA. Cells were lysed two days after transfection and lysates were analyzed by western blotting with indicated antibodies. The custom-made anti-PRG2 antibody shows a dose-dependent reduction of PRG2 in siRNA-mediated knock-down conditions. (**B**) Stainings of *Prg2-WT* as well as *Prg2 -/-* neurons with anti-Tau (blue) and the custom-made anti-PRG2 antibody (green) shows specificity in immunofluorescence. Scale bar: 10 µm. (**C**) Latrunculin treatment (5 µM for 1 hour) affects F-actin content in neurons but does not alter normal neuronal morphology. Images, captured on a Leica TCS SP5 confocal microscope, show representative examples of DIV 9 neurons stained with an anti-α-tubulin antibody and Phalloidin (F-actin). Scale bar: 50 µm. (**D**) Comparison of PRG2 puncta distributions in control and Latrunculin B-treated neurons for 1 h and 3 h (same dataset as in Fig. 4F bar graph). Latrunculin B caused a time-dependent increase in PRG2 puncta frequency with lower co-efficients for Gaussian distribution analysis (control, $R^2 = 0.876$; LatB-1h, $R^2 = 0.698$; LatB-3h, $R^2 = 0.622$). (**E**) Quantification of PRG2 membrane localization as a percentage of plasma membrane puncta vs intra-axonal puncta after 1 and 3 h. Latrunculin B caused a significant net reduction of PRG2 membrane localization after 3 h treatment. $*P < 0.05$, $**P < 0.01$ (t-test).

Supplemental Figure S3

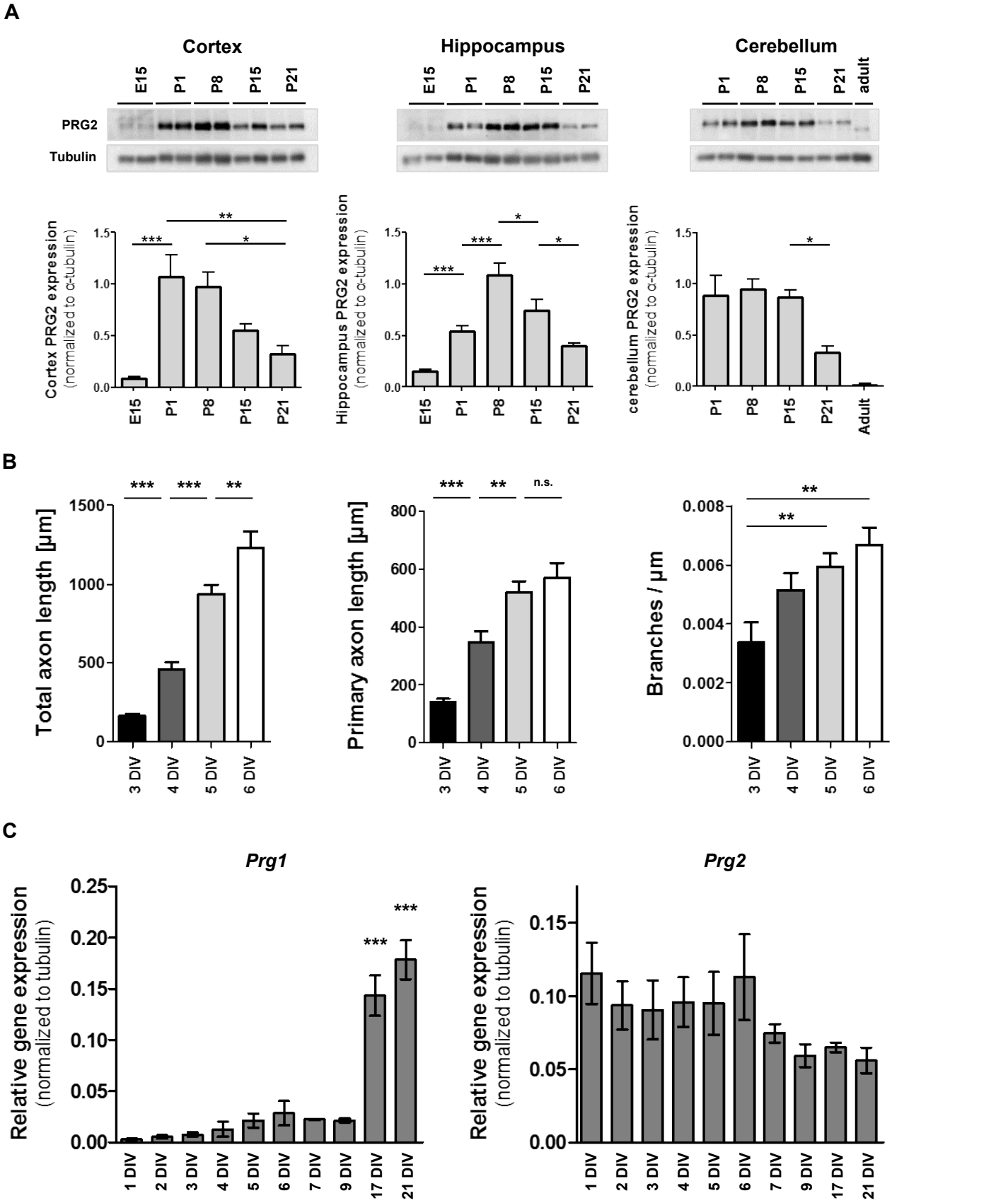

Supplemental Figure S3

***Prg2* expression in vivo and branching in primary cultures, Related to Figure 4**

(**A**) *Prg2* expression rises steeply during early postnatal development of cortex and hippocampus, reaching peaks at postnatal days 1-8, with decreases in expression after postnatal day 15. In cerebellum, expression stays high until postnatal day 15. Bars indicate means ± SEM from n=8 experiments with 3 animals per age and brain region; * P< 0.05, ** P< 0.01, *** $P < 0.001$ (one-way ANOVA with Bonferroni post hoc test). (**B**) Primary cortical neurons grow at a steady rate between three and six days in vitro as indicated by increasing total axon length. The length of the longest process in the axon however seems to plateau indicating that starting after 4 days in vitro, growth mainly is directed into axonal branches. Bars indicate means ± SEM of n=33-51 cells from 3 independent experiments. (**C**) Quantification of relative mRNA abundance of *Prg1* and *Prg2* at different ages indicates a regulation of *Prg1* at the RNA level and *Prg2* at the protein level. Bars represent mean transcript abundance relative to tubulin ± SEM of the 3 independent cultures. *** $P < 0.001$ (one-way ANOVA with Bonferroni post hoc test).

Supplemental Figure S4

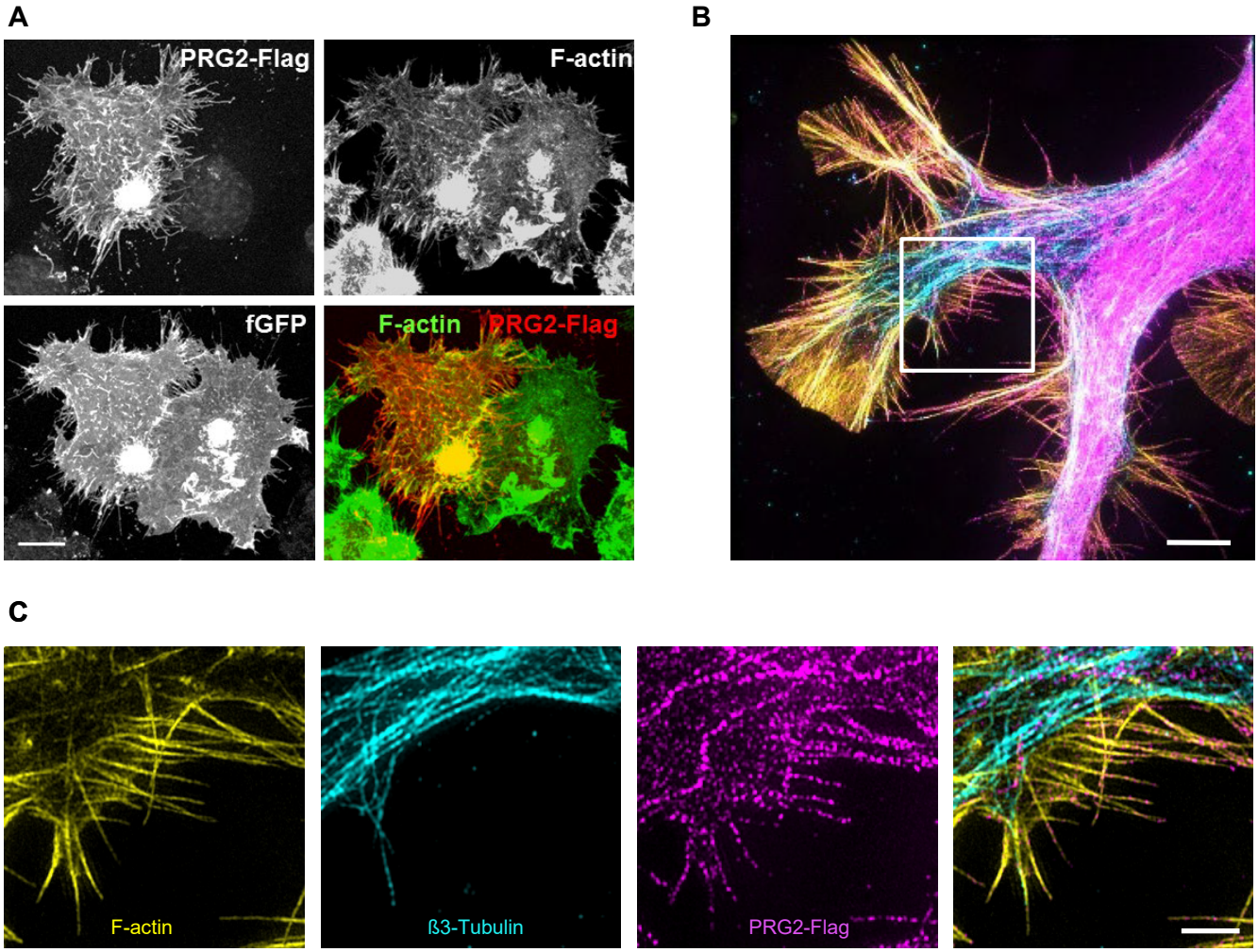

Supplemental Figure S4

PRG2 localizes to filopodia and its overexpression induces the formation of filopodia in N1E-115 neuroblastoma cells, Related to Figure 5

(A) *Prg2-Flag* and farnesylated GFP (*fGFP*) were co-expressed in neuroblastoma cells. PRG2-Flag was visualized using an anti-Flag antibody. Phalloidin labeling visualized the distribution of filamentous actin (F-actin). Scale bar: 10 µm. (**B-C**) Super-resolution SIM analysis of PRG2-Flag localization in N1E cells reveals punctate localization on F-actin rich filopodia as well as endosomal structures. (**B**) overview of N1E cell, scale bar = 5 µm, (**C**) magnification of filopodia, scale bar = 2 µm.

Supplemental Figure S5

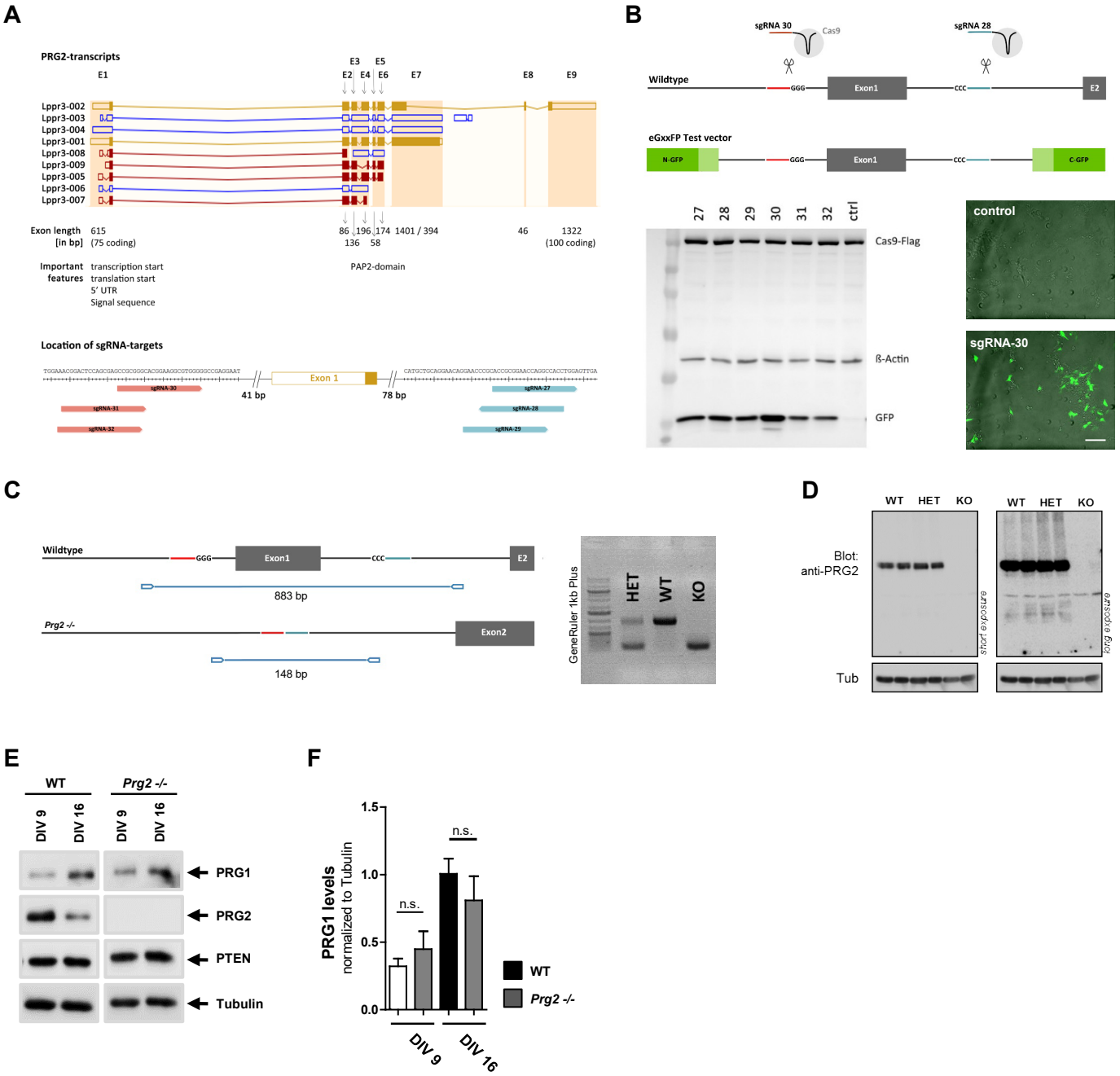

Supplemental Figure S5

Generation of *Prg2 -/-* mice was undertaken using CRISPR/Cas9 mediated Non-homologous end-joining, Related to Figure 6

(**A**) Exon 1 was chosen as the target for CRISPR-mediated excision as it is part of every *Prg2* transcript in the Ensembl-Genome browser and includes the start of translation. Guide-RNAs with minimal predicted off-target effects were chosen in non-coding regions around exon 1. (**B**) Candidate guide RNAs were tested for efficiency (as described in Mashiko et al, 2013) with a plasmid containing overlapping parts of *eGFP* cDNA spaced by the genomic target region of *Prg2*. Efficient Cas9-targeting by guide RNAs results in homologous repair of the *GFP* transcript and therefore *GFP* expression, which was monitored by fluorescence microscopy and western blot. The most efficient guide RNAs and *Cas9* mRNA were synthesized *in vitro,* purified and co-injected into the pro-nucleus and cytosol of single-cell zygotes. Scale bar: 100 µm. (**C**) Offspring were genotyped with primers around exon 1 resulting in a 883 bp (WT) or a 148 bp (*Prg2-/-)* PCR-product respectively. (**D**) Full knockout of *Prg2* was verified by western blotting with anti-PRG2 antibody in whole brain lysate of homozygote *Prg2 -/-* mice. Overexposure shows complete deletion of specific PRG2 signal (i.e. no truncated version of PRG2 is expressed) and an unaffected low-intensity unspecific signal. (**E**) *Prg1* expression is not altered in *Prg2 -/-* primary cortical neurons at DIV9 and DIV16. (**F**) Quantification of PRG1 abundance normalized to tubulin. N=3 independent experiments.

Supplemental Figure S6

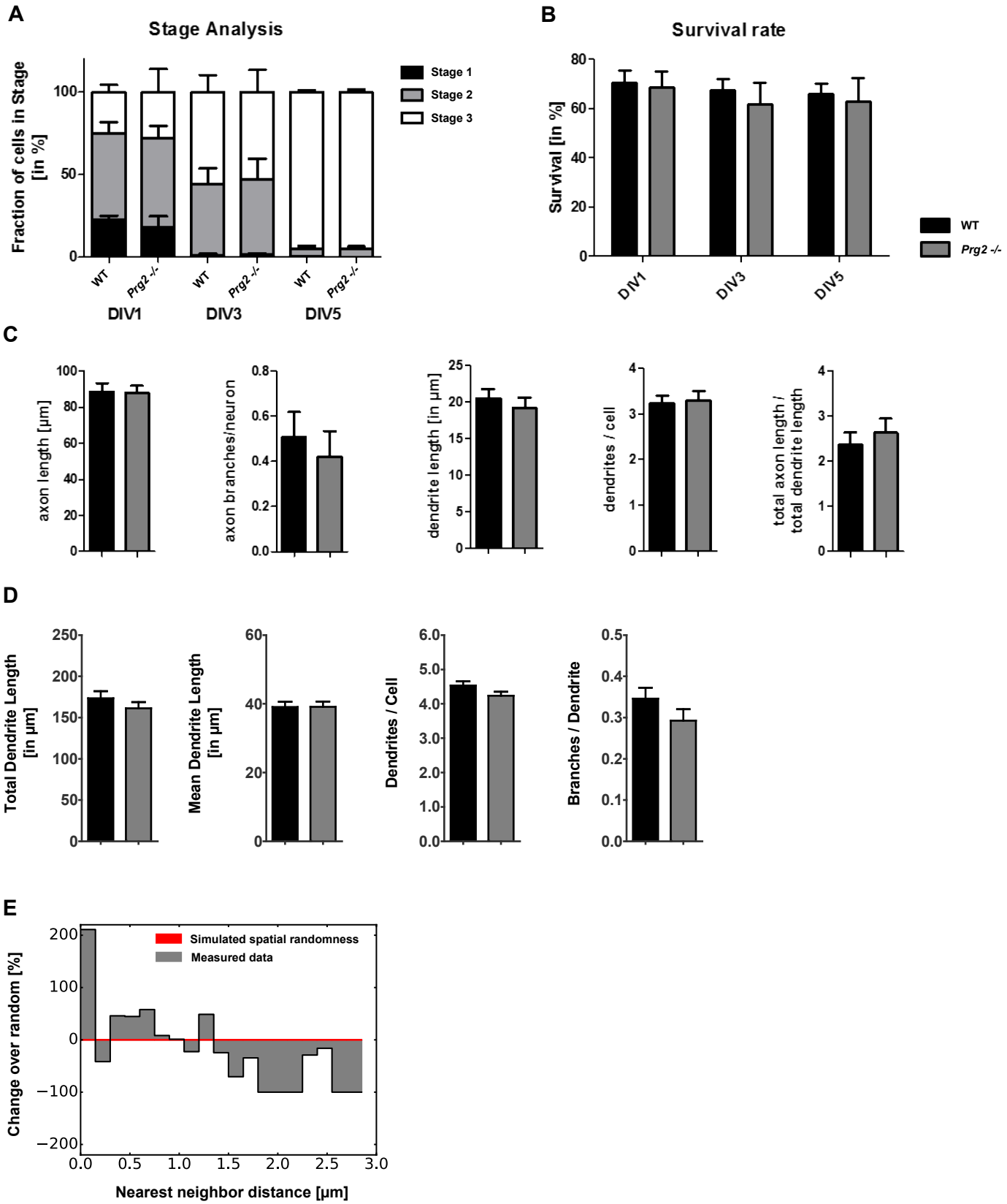

Supplemental Figure S6

Quantification of neuronal morphogenesis and axon filopodia emergence, Related to Figure 6

(**A**) Stage analysis does not reveal differences of *Prg2 -/-* neurons in early development. Bar graphs represent the fraction of neurons in the specified developmental stage at indicated time points ± SEM of 2 independent experiments quantified in 16 images per condition. (**B**) Survival of *Prg2 -/-* neurons is not altered. Bar graphs represent mean survival rate quantified in 16 images per condition by nuclear morphology ± SEM of 2 independent experiments at indicated time points. (**C**) Bar graphs show additional growth parameters quantified from early polarized neurons (1.5 days in culture) shown in Figure 6B as means ± SEM of 4 independent experiments, $n \geq 100$. (**D**) Bar graphs show dendritic growth parameters quantified from stage 3-4 neurons shown in Figure 6D as means ± SEM of 3 independent experiments, $n \geq 100$. (**E**) Nearest neighbor distribution of emerging filopodia to PRG2 clusters relative to randomly distributed clusters (corresponding to Box plot in Fig 6I). Graph shows increased PRG2 abundance at smaller distances and decreased abundance at larger distances to emerging filopodia compared to spatial randomness. Changes of PRG2 appearance were calculated over spatial randomness ([measured data – random] / random). The red line indicates the Bonferroni-corrected 95% confidence interval for each bin calculated from 1000 iterations. n=73 from 4 independent experiments. Bin size: 150nm.

Supplemental Figure S7

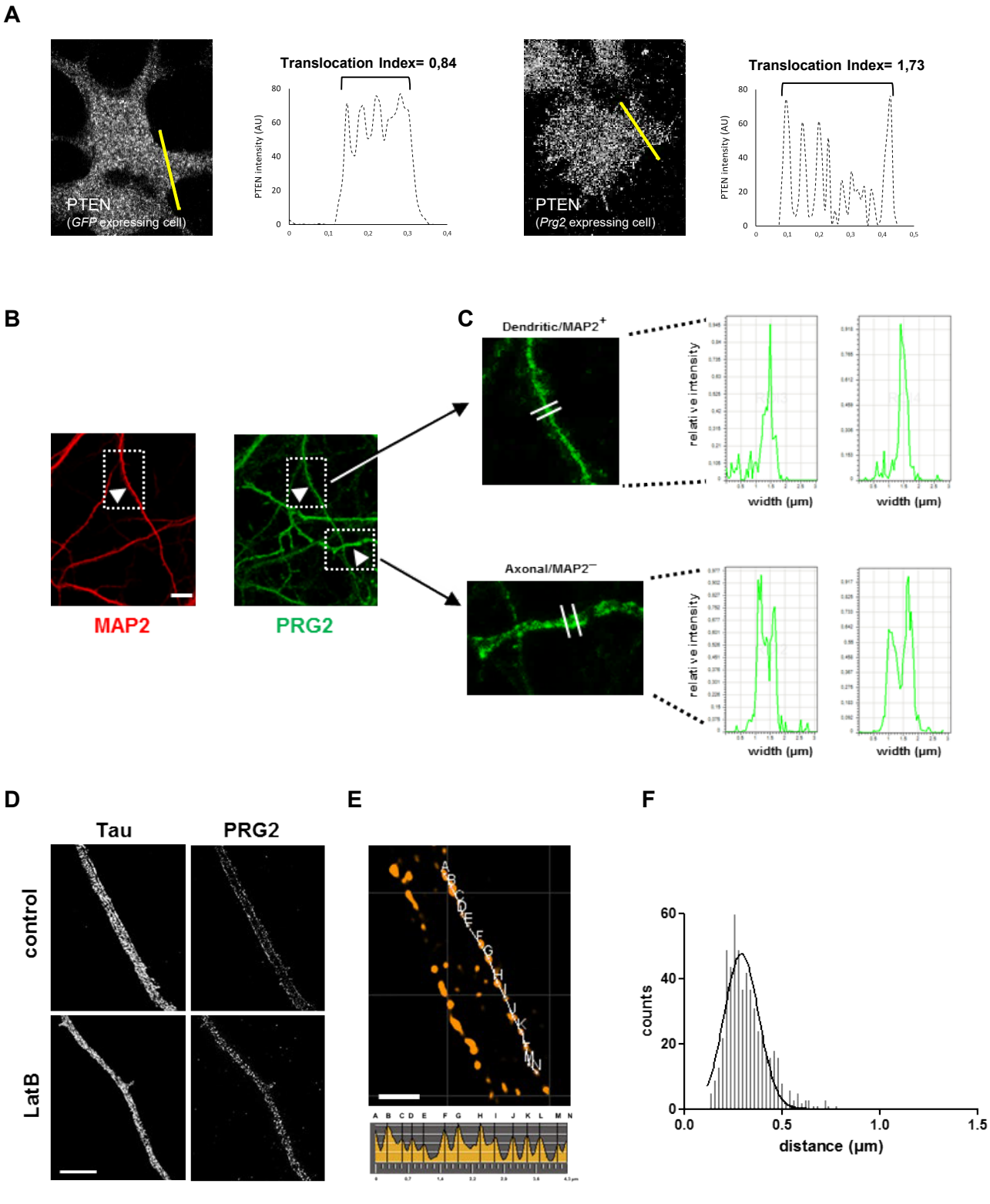

Supplemental Figure S7

Description of custom quantification methods, Related to STAR methods

(**A**) PTEN membrane recruitment was quantified on individual z-planes by drawing lines across the soma of cells, running line intensity profiles and calculating average intensities at the edge (plasma membrane) and cytoplasm of cells. Intensities below a threshold of 3AU were excluded from analysis. PTEN translocation index is the ratio of plasma membrane/cytosol average intensities. (**B**) Analysis of PRG2 localization in axons and dendrites was undertaken by acquiring high magnification images of PRG2-stained hippocampal neurons on a Leica TCS SP5 confocal microscope. Selected processes identified as dendritic (MAP2+, arrowhead) or axonal (MAP2- or Tau+) were then analyzed by LAS AF software using the quantify mode. Scale bar: 5µm. (**C**) We analyzed single stacks of individual processes with similar widths, for PRG2 distribution by drawing vertical lines crossing the process, running line intensity profiles and normalizing intensity values. In the majority of dendritic processes, PRG2 was distributed in a near homogeneous fashion (intensity plots, top row). In the majority of axonal processes, PRG2 was distributed in a bimodal fashion (intensity plots, bottom). PRG2 distribution was calculated as the ratio of maximum peak to maximum valley intensities along these vertical lines; depending on whether the peaks occurred at the edge or the middle of the process; the ratio provides a measure of membrane localization, with values >1 indicating membrane enrichment (Fig.4D, right bar graph). (**D**) Super-resolution SIM analysis of PRG2 localization and puncta distribution on Tau-positive axonal processes of DIV9 hippocampal neurons. Images are single planes of representative stainings (anti-Tau and anti-PRG2) in control and Latrunculin B-treated hippocampal neurons (5 µM for 3 h; as in Fig. 4F), Scale bar: 5 µm. (**E**) High magnification of an axonal segment with PRG2 puncta along the edge/plasma membrane. Line and letters indicate manual tracing and the maxima/puncta detected using Imaris software; bottom panel shows the intensity plot profile along the line. Scale bar: 0.5 µm. (**F**) Frequency distribution of PRG2 puncta in control hippocampal neurons. Distances between consecutive PRG2 puncta were measured along short axonal segments (>1.5 µm) covering a total axonal length of 174 µm. The peak of the distribution is at 260 nm and the mean is 0.292 nm. Analysis suggests a Gaussian distribution ($R^2 = 0.876$).